Spin and charge dynamics in a renormalized perturbation theory

A C Hewson

Department of Mathematics, Imperial College, London SW7 2BZ, UK

E-mail: a.hewson@imperial.ac.uk

Abstract
We calculate the spin and charge dynamical susceptibilities of a strongly correlated impurity model in a renormalized perturbation theory. The irreducible vertices for the quasiparticle scattering are deduced from the renormalized parameters, which have been calculated by fitting the low-lying levels of a numerical renormalization group (NRG) calculation to those of an effective Anderson model. The susceptibilities are asymptotically exact in the low frequency limit and satisfy the Korringa–Shiba relation. By comparing the results with those calculated from a direct NRG calculation, we show that the renormalized perturbation theory (RPT) description gives a very good description of the spin dynamics for all values of the local interaction U, not only at low frequencies but over the whole relevant frequency range.

In the presence of a magnetic field the approach can be generalized using field dependent renormalized parameters to calculate the transverse and parallel spin dynamic susceptibilities. The RPT gives accurate results for the spin dynamics over the whole frequency range and for all values of the magnetic field.

(Some figures in this article are in colour only in the electronic version)

1. Introduction

The scattering of electrons with low energy spin excitations is responsible for the anomalous behaviour of many systems which are described as being strongly correlated. In magnetic impurity systems this scattering is enhanced, leading to the Kondo effect and the many-body resonance (Kondo resonance) which develops at low temperatures at the Fermi level. It is also the origin of the large mass enhancements in heavy fermion systems, and the strong renormalization of the energy bands at the Fermi level. At a quantum critical point, where the critical temperature for magnetic ordering is reduced to zero by pressure or alloying, it is the local low energy fluctuations which cause the breakdown of Fermi liquid theory. In

the cuprate high temperature superconductors, it is the scattering with the spin fluctuations, after the antiferromagnetic order has been destroyed through doping, which is the likely cause of the anomalous electronic behaviour in the normal state. The exchange of the magnetic fluctuations between the conduction electrons may be the origin of the electron attraction leading to superconductivity. It is important, therefore, to understand the nature of these fluctuations in the absence of any long range magnetic order. Here, we study the spin dynamics in a strongly correlated local model, the impurity Anderson model [1], and calculate the local spin dynamics using a renormalized perturbation theory expansion. We start by describing the model and the technical aspects of the approach in this section of the paper, and later present results for various parameter regimes, both with and without an applied magnetic field.

The Anderson model has the form

$$H_{\mathrm{AM}} = \sum_{\sigma} \epsilon_d d_{\sigma}^{\dagger} d_{\sigma} + U n_{d,\uparrow} n_{d,\downarrow} + \sum_{k,\sigma} (V_k d_{\sigma}^{\dagger} c_{k,\sigma} + V_k^* c_{k,\sigma}^{\dagger} d_{\sigma}) + \sum_{k,\sigma} \epsilon_{k,\sigma} c_{k,\sigma}^{\dagger} c_{k,\sigma}, \tag{1}$$

where ϵ_d is the energy of the impurity level, U is the interaction at the impurity site, and V_k the hybridization matrix element to a band of conduction electrons with energy ϵ_k. In the wide band limit the hybridization weighted density of states, $\Delta(\omega) = \pi \sum_k |V_k|^2 \delta(\omega - \epsilon_k)$, can be taken as a constant Δ. With this assumption the impurity one-electron with spin σ Green's function is given by

$$G_{d\sigma}(\omega) = \frac{1}{\omega + \mathrm{i}\Delta - \epsilon_d - \Sigma_{\sigma}(\omega)} \tag{2}$$

where $\Sigma_{\sigma}(\omega)$ is the self-energy.

We have demonstrated in earlier work that the low energy fixed point of this model [2, 3] can be interpreted in terms of the same model but with renormalized parameters [4, 5]. The renormalized model takes the form

$$\tilde{H}_{\mathrm{AM}} = \sum_{\sigma} \tilde{\epsilon}_d d_{\sigma}^{\dagger} d_{\sigma} + \tilde{U} : n_{d,\uparrow} n_{d,\downarrow} : + \sum_{k,\sigma} (\tilde{V}_k d_{\sigma}^{\dagger} c_{k,\sigma} + \tilde{V}_k^* c_{k,\sigma}^{\dagger} d_{\sigma}) + \sum_{k,\sigma} \epsilon_{k,\sigma} c_{k,\sigma}^{\dagger} c_{k,\sigma}, \tag{3}$$

where the colon brackets indicate that the expression within them must be normal-ordered. The three parameters which specify this renormalized model are $\tilde{\epsilon}_d$, $\tilde{\Delta}$ and $\tilde{U}$, defined by

$$\tilde{\epsilon}_d = z(\epsilon_d + \Sigma(0)), \qquad \tilde{\Delta} = z\Delta, \qquad \tilde{U} = z^2 \Gamma_{\uparrow\downarrow}(0, 0, 0, 0), \tag{4}$$

where z is given by $z = 1/(1 - \Sigma'(0))$ and $\Gamma_{\uparrow\downarrow}(\omega_1, \omega_2, \omega_3, \omega_4)$ is the local 4-vertex [4]. The renormalized Hamiltonian (3) describes only the low energy fixed point and the leading irrelevant corrections. A complete description of the original model can be obtained by working in the Lagrangian formulation. The Lagrangian of the original model $\mathcal{L}_{\mathrm{AM}}(\epsilon_d, \Delta, U)$ can be rewritten in terms of the renormalized model plus counter-terms,

$$\mathcal{L}_{\mathrm{AM}}(\epsilon_d, \Delta, U) = \mathcal{L}_{\mathrm{AM}}(\tilde{\epsilon}_d, \tilde{\Delta}, \tilde{U}) + \mathcal{L}_{\mathrm{ct}}(\lambda_1, \lambda_2, \lambda_3), \tag{5}$$

where $\mathcal{L}_{\mathrm{ct}}(\lambda_1, \lambda_2, \lambda_3)$ describes counter-terms. In this formulation a renormalized perturbation expansion can be carried out in terms of the quasiparticle propagators in powers of the renormalized interaction $\tilde{U}$. The role of the three parameters λ_1, λ_2 and λ_3 in the counter-term is to cancel any further renormalization of the parameters, $\tilde{\epsilon}_d$, $\tilde{\Delta}$ and $\tilde{U}$, which are taken to be fully renormalized from the start [4, 5].

In terms of the renormalized parameters the exact results for the impurity spin and charge susceptibilities take a simple form,

$$\chi_{\mathrm{s}} = \tfrac{1}{2} \tilde{\rho}(0)(1 + \tilde{U} \tilde{\rho}(0)), \qquad \chi_{\mathrm{c}} = \tfrac{1}{2} \tilde{\rho}(0)(1 - \tilde{U} \tilde{\rho}(0)), \tag{6}$$
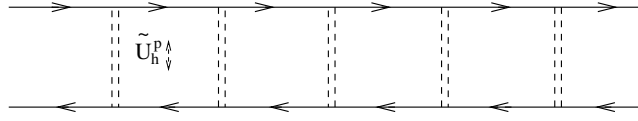
Figure 1. The repeated scattering of a quasiparticle ↑ and a quasihole ↓ which is taken into account in the RPT calculation of the dynamic spin susceptibility $\chi_s(\omega)$.

where $\chi_s(0)$ is in units of $(g\mu_B)^2$, $\chi_c(0)$ differs by a factor from the usual definition, so that, for the non-interacting system, $\chi_c(0) = \chi_s(0)$, and $\tilde{\rho}(\omega)$ is the local density of states for the non-interacting quasiparticles,

$$\tilde{\rho}(\omega) = \frac{\tilde{\Delta}/\pi}{(\omega - \tilde{\epsilon}_d)^2 + \tilde{\Delta}^2}. \tag{7}$$

These results correspond to a first order calculation in the renormalized perturbation expansion in powers of $\tilde{U}$ [4, 6].

We can choose to work solely in terms of the parameters, $\tilde{\epsilon}_d$, $\tilde{\Delta}$ and $\tilde{U}$, and determine them by comparison with experiments, as one does in a phenomenological Fermi liquid theory. To determine them in terms of the bare parameters of the original model using equation (4) it would seem that we need almost the complete solution of the model, including the dynamics. However, they can be calculated without recourse to these formulae by fitting the low energy excitations of the numerical renormalization group calculations to those of the effective low energy model given in equation (3), as was done essentially in the original NRG calculations [2, 3]. The results for $\tilde{\epsilon}_d$, $\tilde{\Delta}$ and $\tilde{U}$, for various parameter regimes of the model, have been described in earlier work [7].

We wish to generalize the results for the spin and charge susceptibilities given in equation (6) to obtain the corresponding dynamic susceptibilities: the spin susceptibility, $\chi_s(\omega)$, which is given by the Fourier transform of the double-time Green's functions of either $\langle\langle d_\uparrow^\dagger(t)d_\downarrow(t); d_\downarrow^\dagger(t')d_\uparrow(t')\rangle\rangle/2$ (transverse susceptibility), or $\langle\langle n_{d\uparrow}(t) - n_{d\downarrow}(t); n_{d\uparrow}(t') - n_{d\downarrow}(t')\rangle\rangle/4$ (parallel susceptibility), as they are equal in the absence of a magnetic field, and the charge susceptibility, $\chi_c(\omega) = \langle\langle n_{d\uparrow}(t) + n_{d\downarrow}(t) : n_{d\uparrow}(t') + n_{d\downarrow}(t')\rangle\rangle/4$. To calculate these we need to look at the processes involving repeated quasiparticle scattering. A typical diagram in the renormalized perturbation expansion corresponding to the repeated scattering of a spin up quasiparticle with a spin down quasihole is shown in figure 1. These scattering terms at $\omega = 0$ have implicitly been taken into account in the results for the static susceptibilities in (6), and so we must introduce the counter-term λ_3 to prevent overcounting. We define an irreducible interaction vertex $\tilde{U}_{h\downarrow}^{p\uparrow} = \tilde{U} - \lambda_3$, and sum the series to derive an expression for the dynamic spin susceptibility,

$$\chi_s(\omega) = \frac{1}{2} \frac{\tilde{\Pi}_{h\downarrow}^{p\uparrow}(\omega)}{1 - \tilde{U}_{h\downarrow}^{p\uparrow}\tilde{\Pi}_{h\downarrow}^{p\uparrow}(\omega)}, \tag{8}$$

where $0.5\tilde{\Pi}_{h\downarrow}^{p\uparrow}(\omega)$ is the spin dynamic charge susceptibility for the non-interacting quasiparticles. Expressions for $\tilde{\Pi}_{h\downarrow}^{p\uparrow}(\omega)$ for the particle–hole symmetric model are given in the appendix. The approach is similar to the random phase approximation (RPA) in terms of quasiparticles [8, 9] and goes over to the RPA expression in the weak coupling limit.
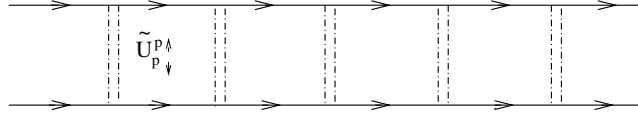
Figure 2. The repeated scattering of a quasiparticle $\uparrow$ and a quasiparticle $\downarrow$ which is summed in the RPT calculation of the dynamic charge susceptibility $\chi_c(\omega)$.

At zero frequency we can identify the result with the spin susceptibility given in equation (6),

$$\chi_s(0) = \frac{1}{2} \frac{\tilde{\rho}(0)}{1 - \tilde{U}_{h\downarrow}^{p\uparrow}\tilde{\rho}(0)} = \frac{\tilde{\rho}(0)}{2}(1 + \tilde{U}\tilde{\rho}(0)). \tag{9}$$

The effective particle–hole vertex can then be deduced in terms of $\tilde{U}$,

$$\tilde{U}_{h\downarrow}^{p\uparrow} = \frac{\tilde{U}}{1 + \tilde{U}\tilde{\rho}(0)}. \tag{10}$$

In terms of conventional Landau Fermi liquid notation, $\tilde{\rho}(0)\tilde{U}_{h\downarrow}^{p\uparrow} = -F_0^a$. The resulting expression for $\chi_s(\omega)$ in terms of $\tilde{U}$ is

$$\chi_s(\omega) = \frac{1}{2} \frac{\tilde{\Pi}_{h\downarrow}^{p\uparrow}(\omega)(1 + \tilde{U}\tilde{\rho}(0))}{1 + \tilde{U}\tilde{\rho}(0) - \tilde{U}\tilde{\Pi}_{h\downarrow}^{p\uparrow}(\omega)}. \tag{11}$$

This result is asymptotically exact as $\omega \to 0$ as $\chi_s(\omega) \to \tilde{\rho}(0)(1 + \tilde{U}\tilde{\rho}(0))/2$ (by construction), and its imaginary part satisfies the Korringa–Shiba relation,

$$\lim_{\omega \to 0} \frac{\text{Im}\,\chi_s(\omega)}{\pi\omega} = \frac{\tilde{\rho}^2(0)}{2}(1 + \tilde{U}\tilde{\rho}(0))^2 = 2\chi_s^2(0), \tag{12}$$

which is an exact relation for the Anderson model [11]. We note that the result (11), in the large U limit where $\tilde{U}\tilde{\rho}(0) \to 1$, is equivalent to that derived by Kuramoto and Miyake [12] based on a semi-phenomenological Fermi liquid theory.

We repeat this exercise but this time consider the repeated scattering of two quasiparticles of opposite spin, as illustrated in figure 2, and define a corresponding irreducible interaction vertex $\tilde{U}_{p\downarrow}^{p\uparrow}$. The sum of this series gives, for the charge dynamic susceptibility,

$$\chi_c(\omega) = \frac{2\tilde{\Pi}_{p\downarrow}^{p\uparrow}(\omega)}{1 - \tilde{U}_{p\downarrow}^{p\uparrow}\tilde{\Pi}_{h\downarrow}^{p\uparrow}(\omega)}. \tag{13}$$

Identifying the $\omega = 0$ result with the charge susceptibility in equation (6),

$$\chi_c(0) = \frac{1}{2} \frac{\tilde{\rho}(0)}{1 - \tilde{U}_{p\downarrow}^{p\uparrow}\tilde{\rho}(0)} = \frac{\tilde{\rho}(0)}{2}(1 - \tilde{U}\tilde{\rho}(0)). \tag{14}$$

The effective particle–particle vertex can then be deduced in terms of $\tilde{U}$,

$$\tilde{U}_{p\downarrow}^{p\uparrow} = \frac{\tilde{U}}{1 - \tilde{U}\tilde{\rho}(0)}. \tag{15}$$

In terms of conventional Landau Fermi liquid notation, $\tilde{\rho}(0)\tilde{U}_{p\downarrow}^{p\uparrow} = F_0^s$, and the values of F_0^s and F_0^a are such as to satisfy the forward scattering sum rule [10],

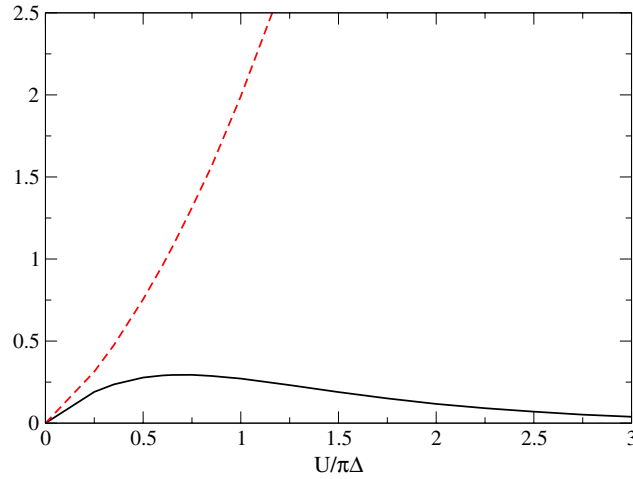$$\frac{F_0^s}{1 + F_0^s} + \frac{F_0^a}{1 + F_0^a} = 0. \tag{16}$$

Figure 3. The irreducible vertices, $\tilde{U}_{h\downarrow}^{p\uparrow}$ (full line) and $\tilde{U}_{p\downarrow}^{p\uparrow}$ (dashed line), as a function of $U/\pi\Delta$ for the symmetric Anderson model.

In figure 3 we give the two irreducible vertices, $\tilde{U}_{h\downarrow}^{p\uparrow}/\pi\Delta$ and $\tilde{U}_{p\downarrow}^{p\uparrow}/\pi\Delta$, for the symmetric Anderson model as a function of $U/\pi\Delta$. It can be seen that there is a rapid divergence between the interactions in the spin and charge channels with increasing U. The vertex $\tilde{U}_{h\downarrow}^{p\uparrow}$ in the spin channel decreases monotonically with increase of U and in the limit of large U it tends to the value $2T_K$, where T_K is the Kondo temperature given by $T_K = \sqrt{(U\Delta/2)}e^{-\pi U/8\Delta+\pi\Delta/2U}$. The vertex $\tilde{U}_{p\downarrow}^{p\uparrow}$ in the charge channel, on the other hand, increases monotonically though it remains finite and diverges only in the limit $U \to \infty$.

The RPT result for the dynamic charge susceptibility is

$$\chi_c(\omega) = \frac{1}{2}\frac{\tilde{\Pi}_{h\downarrow}^{p\uparrow}(\omega)(1 - \tilde{U}\tilde{\rho}(0))}{1 - \tilde{U}\tilde{\rho}(0) + \tilde{U}\tilde{\Pi}_{h\downarrow}^{p\uparrow}(\omega)}, \tag{17}$$

where $\tilde{\Pi}_{p\downarrow}^{p\uparrow}(\omega)$ for the symmetric model is given in the appendix. This result is again asymptotically exact and satisfies the relevant Korringa–Shiba relation. In the next sections we evaluate these expressions for the particle–hole symmetric model, and compare the results with those calculated directly from numerical renormalization group calculations.

2. Dynamic susceptibilities in the absence of a magnetic field

We have shown that the RPT expressions for $\chi_s(\omega)$ and $\chi_c(\omega)$ are asymptotically exact in the limit $\omega \to 0$, but we would like to know over what range of finite ω they give accurate results. To estimate this we compare them with the corresponding results derived from a direct numerical renormalization group (NRG) calculation for the dynamics [13, 14]. These spectra can be calculated using the same methods which have been developed for calculating the spectral density of the one-electron impurity Green's function. These direct calculations give a good overall picture of the behaviour over all energy scales, but have some inaccuracies stemming mainly from the use of a discrete spectrum for the conduction electrons, and the logarithmic broadening which is used to give the final continuous spectrum. To gauge the accuracy of the direct NRG calculations we calculate $\chi_s(\omega)$ using this technique for the non-interacting system ($U = 0$) and which we can then compare with the exact result which for the
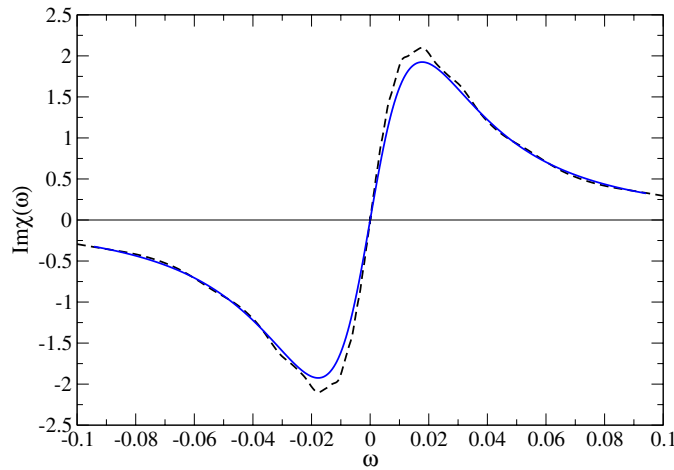
Figure 4. A comparison of the results of an NRG calculation (dashed line) of the imaginary part of the spin susceptibility $\chi_s(\omega)$ for the non-interacting symmetric Anderson model ($U = 0$) compared with an evaluation of the exact result (full line).

particle–hole symmetric model corresponds to equations (11) and (17) with $\tilde{U} = 0$, $\tilde{\epsilon}_d = 0$ and $\tilde{\Delta} = \Delta$. We take $\Delta = 0.015\,708$ for these and all subsequent calculations.

The results for the imaginary part of the retarded susceptibility, Im $\chi_s(\omega)$, are shown in figure 4. We see that the direct NRG results give a reasonably good representation of the overall behaviour. However, there is some overestimate of the gradient at $\omega = 0$, leading to a 10% error in the Korringa–Shiba relation, and about a 5% overestimate of the peak height.

We can now make a comparison of the direct NRG results in the interacting case with the corresponding RPT results. We look at a strong correlation situation first of all with $U/\pi\Delta = 3.0$, in which the low energy charge excitations are almost completely suppressed. The values of $\tilde{U}$ and $\tilde{\Delta}$ are calculated from the NRG levels as described in earlier work. The results for Im $\chi_s(\omega)$ are shown in figure 5. The peak structure is very much enhanced compared with the non-interacting case and occurs on a scale $\omega \sim \tilde{\Delta} = 4T_K/\pi$, where T_K is the Kondo temperature. There is very good agreement between the two sets of results over the whole range of this low-lying peak structure. It would appear that the RPT results may be in fact more accurate than the direct NRG results, as they satisfy the Korringa–Shiba relation exactly and, as we saw from the results in figure 4, the direct NRG results tend to overestimate the peak heights. The results for the real part of $\chi_s(\omega)$ are shown in figure 6 and there is good agreement between the results but the direct NRG underestimates the value of $\chi_s(0)$ by about 4%. The corresponding dynamic charge susceptibilities are very small over this range.

We take a smaller value of U such that $U/\pi\Delta = 1.0$ to see spin and charge peaks of the same order. The NRG and RPT results for both Im $\chi_s(\omega)$ and Im $\chi_c(\omega)$ are shown in figure 7. The enhancement of the spin peaks are down by a factor of 10 from the strong correlation case shown in figure 5, and the ω range shown is greater by the same factor. In this moderately correlated case the peaks in the charge spectrum are reduced but can be seen on the same scale as the spin peaks. Again there is very good agreement between the NRG and RPT results over this whole range, and the evidence from the earlier results suggests that the RPT results may be the more accurate ones over this range.

We take a case of weak correlation with $U/\pi\Delta = 0.5$. In this case it should be meaningful to make a comparison with the standard RPA results, which correspond to taking the bare
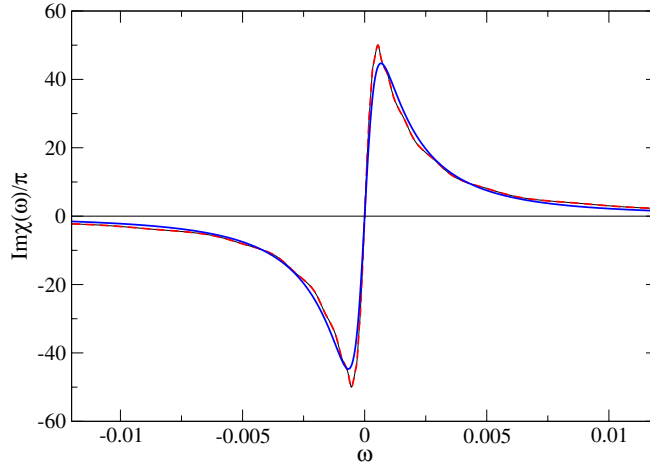
Figure 5. Results for the imaginary part of the dynamic spin susceptibility $\chi_s(\omega)/\pi$ for the symmetric model in the Kondo regime $U/\pi\Delta = 3.0$. The dashed curve corresponds to the NRG results and the full line to the results using the RPT expression, equation (11).
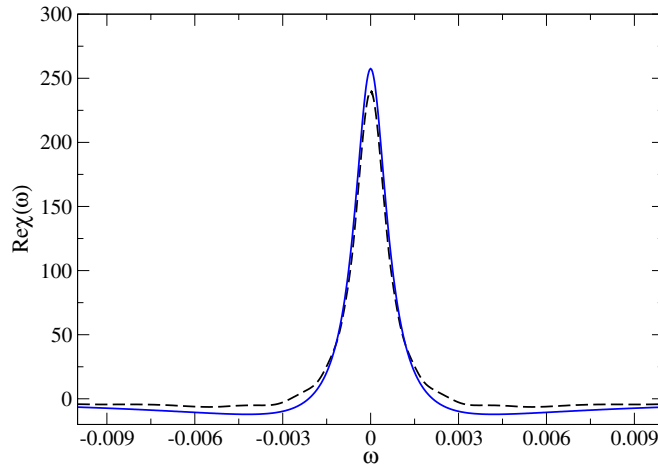

Figure 6. Results for the real part of the dynamic spin susceptibility $\chi_s(\omega)$ for the symmetric model in the Kondo regime $U/\pi\Delta = 3.0$. The dashed curve corresponds to the NRG results and the full line to the results using the RPT expression, equation (11).

parameters in the RPT formulae; $U_{h\downarrow}^{p\uparrow} = U$, $\tilde{\Delta} = \Delta$. The results of all three calculations for the imaginary part of the dynamic spin susceptibility are shown in figure 8. All three curves are qualitatively similar, and there is very good agreement between them regarding the peak positions. The differences between the NRG and RPT results are similar to those noted in figures 4 and 6. If we compare the peaks with those in the non-interacting case shown in figure 4, we see that they are enhanced only by a factor of the order 1.5. The peak heights are overestimated in the RPA results.

In figure 9 we present the results for Im $\chi_s(\omega)/\pi\chi_s^2(0)$, for the four sets of results $U/\pi\Delta = 0.0, 0.5, 1.0, 3.0$. All sets have the value 2 at $\omega = 0$, corresponding to the
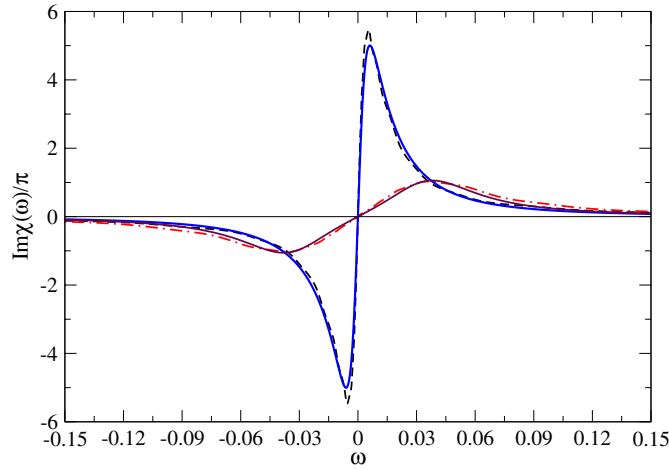
Figure 7. Results for the imaginary parts of both the dynamic spin $\chi_s(\omega)$ and charge susceptibilities $\chi_c(\omega)$ for the symmetric model with $U/\pi\Delta = 1.0$. The dashed curve (spin) and the dot–dashed curve (charge) correspond to the NRG results and the full lines (thick: spin; thin: charge) to the results using the RPT expressions.
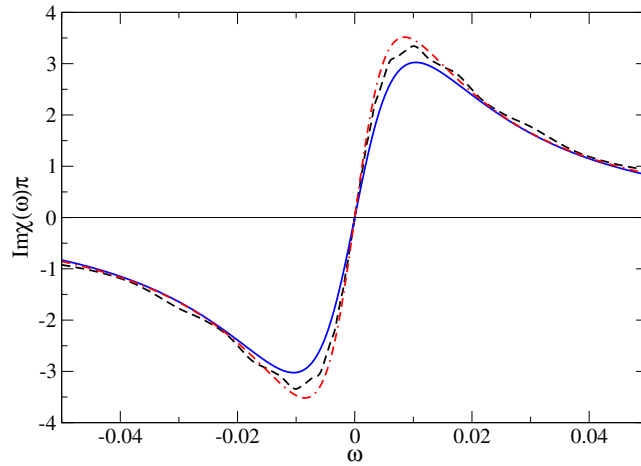

Figure 8. The imaginary part of the dynamic spin susceptibility for a weak correlation case of the symmetric model with $U/\pi\Delta = 0.5$. The three sets of results are from (i) NRG calculations (dashed line), (ii) RPT (full line) and (iii) RPA (dot–dashed line).

Korringa–Shiba relation. With increasing U there is the same narrowing to a scale set by the Kondo temperature as in the one-electron spectral density of the impurity Green's function. Combining the Kramers–Kronig relation, $\int_{-\infty}^{\infty} \mathrm{Im}\chi(\omega)/\omega\,\mathrm{d}\omega = \pi\,\mathrm{Re}\,\chi(0)$, with the Korringa–Shiba relation gives

$$\frac{1}{\pi\,\chi_{s,c}^2(0)}\int_{-\infty}^{\infty}\frac{\mathrm{Im}\,\chi_{s,c}(\omega)}{\omega}\,\mathrm{d}\omega = \frac{1}{\chi_{s,c}(0)} = \frac{2\pi\,\tilde{\Delta}}{(1\pm\tilde{U}/\pi\,\tilde{\Delta})}. \tag{18}$$

The total weight under the peak in figure 9, therefore, when $U/\pi\Delta \gg 1$ and $\tilde{U}/\pi\,\tilde{\Delta} \to 1$, is equal to $4T_K$. The sum rule (18) is satisfied precisely in the results shown.
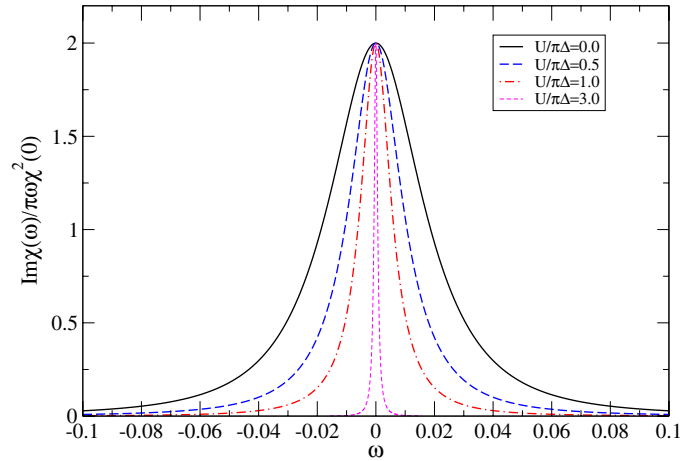
Figure 9. Results for Im $\chi_s(\omega)/\pi\,\chi_s^2(0)$ calculated using the RPT for the symmetric model and a range of values of U.
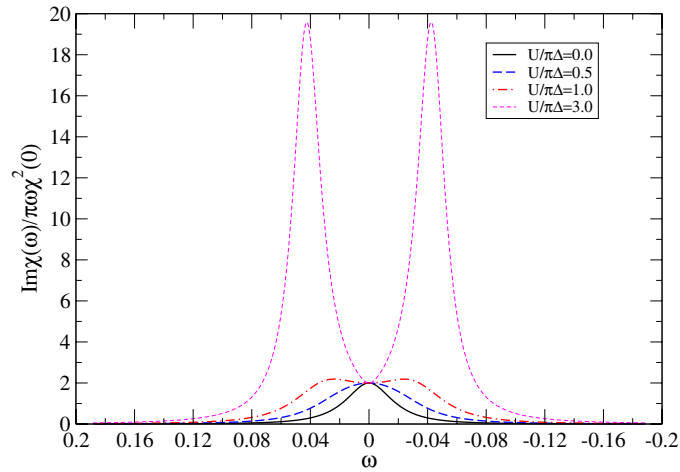

Figure 10. Results for Im $\chi_c(\omega)/\pi\,\chi_s^2(0)$ calculated using the RPT for the symmetric model and the same range of values of U as for the spin susceptibility results shown in figure 9.

These results contrast to the corresponding results for the dynamic charge susceptibility shown in figure 10. Again due to the Korringa–Shiba relation all sets have the value of 2 at $\omega = 0$. The suppression of the charge fluctuations in this case is indicated by the development of symmetric high energy peaks, with values very much greater than the value at $\omega = 0$. From equation (18) it can be seen that as $U \to \infty$ and $\tilde{U}/\pi\,\tilde{\Delta} \to 1$ the area under the curves diverges in this limit. However, though qualitatively correct the RPT restricted to this class of diagrams cannot accurately describe the behaviour on this high energy scale.

3. Dynamic susceptibilities in a magnetic field

We now consider the dynamic spin response for the symmetric model in the presence of an applied magnetic field H. The low energy behaviour can still be described by a renormalized
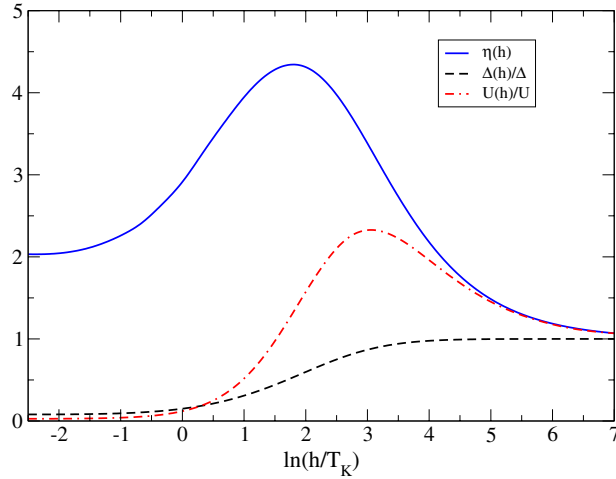
Figure 11. The field dependence of the ratio of the renormalized parameters relative to their bare values, $\eta(h) = \tilde{h}/h$, $\tilde{\Delta}(h)/\Delta$ and $\tilde{U}(h)/U$ for $U/\pi\Delta = 3.0$ plotted as a function of $\ln(h/T_K)$.

Anderson model with parameters which now depend on the magnetic field [15]. The field dependent parameters $\tilde{h}$, $\tilde{\Delta}(h)$ and $\tilde{U}(h)$, are defined by

$$\tilde{h} = z(h)\left(-\frac{U}{2} + \Sigma(0, h)\right), \qquad \tilde{\Delta}(h) = z(h)\Delta, \qquad \tilde{U}(h) = z^2(h)\Gamma_{\uparrow\downarrow}(0, 0, 0, 0 : h),$$
(19)

where $z(h)$ is given by $z(h) = 1/(1 - \Sigma'(0, h))$ and $h = g\mu_B H/2$. These parameters can again be determined from the levels of an NRG calculation [15, 16]. The induced impurity magnetization $M_d(h) = (g\mu_B)^2 m(h)$ at $T = 0$, where $m(h)$ is given exactly by

$$m(h) = \frac{1}{\pi}\tan^{-1}\left(\frac{\tilde{h}(h)}{\tilde{\Delta}(h)}\right),$$
(20)

a result which follows from the Friedel sum rule [17]. The renormalized parameters, $\tilde{\eta}(h) = \tilde{h}/h$, $\tilde{\Delta}(h)$ and $\tilde{U}(h)$, in the presence of a magnetic field H, relative to their bare values, for $U/\pi\Delta = 3.0$ are given in figure 11. The parameters are not all independent and $\tilde{U}(h)$ can be deduced from the other two parameters from the equation [16]

$$1 + \tilde{U}(h)\tilde{\rho}(0, h) = \tilde{\eta}(h) + h\frac{\partial\tilde{\eta}(h)}{\partial h} - \frac{h\tilde{\eta}(h)}{\tilde{\Delta}(h)}\frac{\partial\tilde{\Delta}(h)}{\partial h},$$
(21)

where $\tilde{\rho}(\omega, h)$ is the quasiparticle density of states in the presence of the magnetic field and is given by

$$\tilde{\rho}(\omega, h) = \frac{\tilde{\Delta}(h)/\pi}{(\omega - \tilde{h}(h))^2 + \tilde{\Delta}^2(h)}.$$
(22)

As the magnetic field increases the parameters change from the Kondo regime ($h < T_K$), where $\tilde{\eta}(h) = 2$, and $\tilde{U}(h)\tilde{\rho}(0, h) = 1$, through a local moment regime ($h > T_K$), where $\tilde{\eta}(h)$ increases with h, and $\tilde{U}(h)$ is enhanced to values greater than the bare value U, and finally to the almost free model when $h > U$, and the parameters revert to their bare values.

With a magnetic field present we have to distinguish between the parallel and transverse spin susceptibilities, $\chi_{s,\parallel}(\omega, h)$ and $\chi_{s,\perp}(\omega, h)$. The static values at $T = 0$ are given exactly

by

$$\chi_{s,\parallel}(0,h) = \tfrac{1}{2}\tilde{\rho}(0,h)(1 + \tilde{U}(h)\tilde{\rho}(0,h)), \qquad \chi_{s,\perp}(0,h) = \frac{m(h)}{2h} = \frac{1}{2\pi h}\tan^{-1}\left(\frac{\tilde{h}(h)}{\tilde{\Delta}(h)}\right).$$

(23)

To calculate the frequency dependence of these spin response functions from the quasiparticle scattering we need to calculate the corresponding irreducible particle–hole vertices again as they will now depend on the value of the magnetic field. The transverse susceptibility corresponding to an excitation with a change in the z-component of the impurity spin of 1 involves the scattering of a quasiparticle with spin up with a quasihole with spin down, and the irreducible vertex in this channel we denote by $\tilde{U}_{h\downarrow}^{p\uparrow}(h)$. We derive its value using the same type of argument as earlier by requiring that the sum of the series for $\omega = 0$ should equal the transverse static susceptibility given in equation (23). We obtain the result

$$\tilde{U}_{h\downarrow}^{p\uparrow}(h) = \frac{\pi h(\tilde{\eta}(h) - 1)}{\tan^{-1}(\tilde{h}(h)/\tilde{\Delta}(h))}.$$

(24)

Using the results,

$$\lim_{h\to 0}(\tilde{\eta}(h) - 1) = \tilde{U}\tilde{\rho}(0) = \frac{\tilde{U}}{\pi\tilde{\Delta}}, \qquad \lim_{h\to 0}\frac{\tan^{-1}(\tilde{h}(h)/\tilde{\Delta}(h))}{h} = 1 + \tilde{U}\tilde{\rho}(0),$$

(25)

it can be shown that $\tilde{U}_{h\downarrow}^{p\uparrow}(h)$ goes over to the earlier result in equation (10) in the limit $h \to 0$. The resulting expression for $\chi_{s,\perp}(\omega,h)$ is as given in equation (11) with the h-dependence included in both the scattering vertex $\tilde{U}_{h\downarrow}^{p\uparrow}(h)$ and $\tilde{\Pi}_{h\downarrow}^{p\uparrow}(\omega)$.

The parallel dynamic susceptibility corresponds to repeated scattering of a quasiparticle with spin σ and a quasihole with the same spin component σ, and hence no change in the z-component of the spin. We denote the corresponding irreducible vertex by $\tilde{U}_{h\uparrow}^{p\uparrow}(h)$, corresponding to $\sigma = \uparrow$, but for the symmetric model it is the same as that for $\sigma = \downarrow$. As the static parallel susceptibility has the same form as given earlier in equation (6), apart for the h-dependence, the result is

$$\tilde{U}_{h\uparrow(p\downarrow)}^{p\uparrow}(h) = \frac{\tilde{U}(h)}{(1 \pm \tilde{U}(h)\tilde{\rho}(0,h))},$$

(26)

with the corresponding result for the particle–particle vertex. Using the results from figure 11, we can deduce the three types of vertices as a function of $h/\pi\Delta$ for $U/\pi\Delta = 3.0$. The results are shown in figure 12. Initially for small h, $\tilde{U}_{h\downarrow}^{p\uparrow}(h) = \tilde{U}_{h\uparrow}^{p\uparrow}(h) = 2T_K$, and then they slowly diverge with $\tilde{U}_{h\downarrow}^{p\uparrow}(h) > \tilde{U}_{h\uparrow}^{p\uparrow}(h)$, but converge again for $h > U$ to the bare value U. The charge susceptibility, which is initially very large, decreases and converges to the bare value U for $h > U$.

The transverse dynamic spin susceptibility is antisymmetric in the absence of a field, $\text{Im}\,\chi_{s,\perp}(\omega,0) = -\text{Im}\,\chi_{s,\perp}(-\omega,0)$, as can be seen in the results in figures 4–8, and as a consequence the total integrated spectral weight is zero. This is no longer the case when $h \neq 0$, and the total spectral weight $w_\perp(h)$ is equal to the average z-component of the impurity spin $m(h) = 0.5\langle n_{d\uparrow} - n_{d\downarrow}\rangle$. At $T = 0$ the RPT result for $\chi_{s,\perp}(\omega,h)$ satisfies this result exactly as

$$w_\perp(h) = \lim_{\omega\to\infty}\omega\chi_{s,\perp}(\omega,h) = 0.5\lim_{\omega\to\infty}\omega\tilde{\Pi}_{h\downarrow}^{p\uparrow}(\omega,h) = \frac{1}{\pi}\tan^{-1}\left(\frac{\tilde{h}}{\tilde{\Delta}}\right), \quad (27)$$
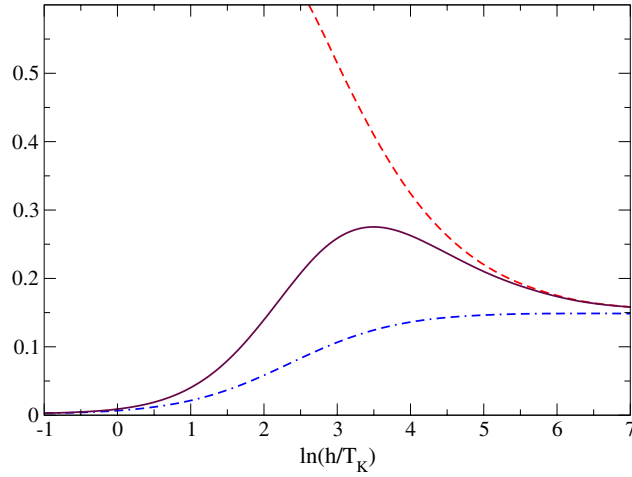
which is equal to $m(h)$ from equation (20).

Figure 12. The irreducible vertices, $\tilde{U}_{h\downarrow}^{p\uparrow}(h)$ (full line), $\tilde{U}_{h\uparrow}^{p\uparrow}(h)$ (dot–dashed line), and $\tilde{U}_{p\downarrow}^{p\uparrow}(h)$ (dashed line) as a function of $\ln(h/T_K)$ for $U/\pi\Delta = 3.0$.
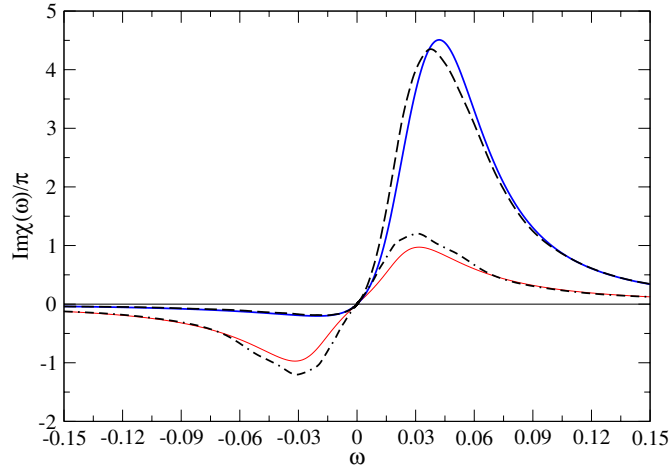

Figure 13. The NRG results for the imaginary parts of $\chi_{s,\perp}(\omega, h)$ (dashed line) and $\chi_{s,\parallel}(\omega, h)$ (dot–dashed) as a function of ω for $U = 0$ compared with the exact results ($\perp$: thick full line; $\parallel$: thin full line) for $h = 0.4\pi\Delta$.

The total spectral weight $w_\parallel(h)$ for the parallel susceptibility $\chi_{s,\parallel}(\omega, h)$ on the other hand vanishes as

$$w_\parallel(h) = \lim_{\omega\to\infty} \omega\chi_{s,\parallel}(\omega, h) = 0.5 \lim_{\omega\to\infty} \omega\tilde{\Pi}_{h\uparrow}^{p\uparrow}(\omega, h) = 0. \tag{28}$$

To gauge the errors in the NRG results[1] due to the use of a discrete spectrum and logarithmic broadening we again compare them with exact results for $U = 0$. The results of this comparison for $h = 0.4\Delta$ are shown in figure 13. We see that the NRG results give the correct overall forms for the imaginary parts for both the transverse and parallel susceptibilities.

[1] In the NRG calculations in the presence of a magnetic field we adopt the density matrix modified NRG approach introduced by Hofstetter [18].
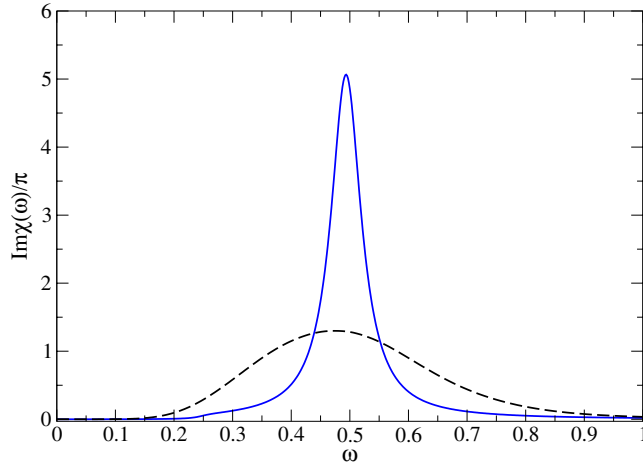
Figure 14. The NRG results for the imaginary parts of $\chi_{s,\perp}(\omega, h)$ (dashed line) and as a function of ω for $U = 0$ compared with the exact results (full line) for $h = 5\pi\Delta$.
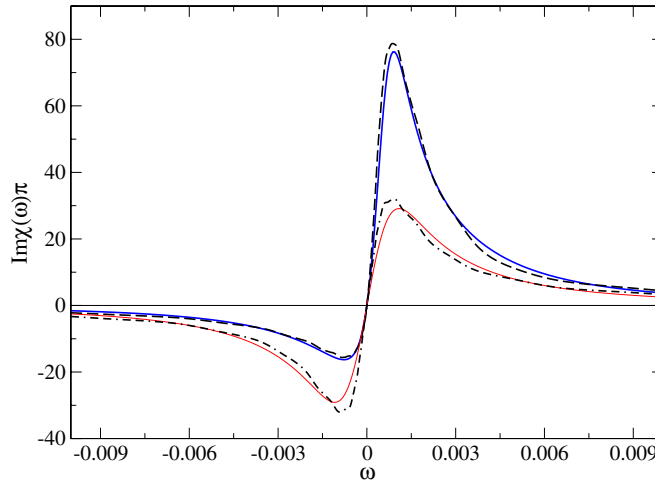

Figure 15. The RPT results for the imaginary parts of $\chi_{s,\perp}(\omega, h)$ (thick full line) and $\chi_{s,\parallel}(\omega, h)$ (thin full line) for $h = 0.4T_{\mathrm{K}}$ as a function of ω for $U/\pi\Delta = 3.0$ compared with the NRG results ($\perp$: dashed line; $\parallel$: dot–dashed line).

However, due to the discrete spectrum and broadening on this relatively high energy scale, there is some deviation from the exact results. The asymmetry of the results for the transverse case due to the field is apparent. In figure 14 we compare the NRG results for the imaginary part of the transverse susceptibility with the exact results for an extremely large magnetic field $h = 5\Delta$. On this scale the impurity is effectively an almost localized and nearly fully polarized local moment. The spectrum, therefore, consists of a single peak at the energy required to flip the spin in the applied field, $\omega_p \sim 2h$. Whereas the exact result has a sharp peak the NRG result is much broader on this high energy scale, but the peak position and total spectral weight of the NRG result are correct.

We now compare the NRG results with those of the RPT results in the strong coupling case corresponding to the Kondo limit. In figure 15 we compare the imaginary parts of the
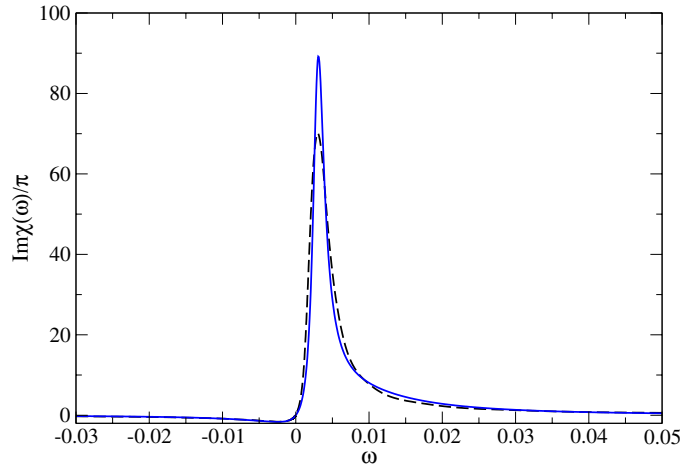
Figure 16. The RPT results for the imaginary parts of $\chi_{s,\perp}(\omega, h)$ (thick full line) for $h = 2T_K$ as a function of ω for $U/\pi\Delta = 3.0$ compared with the NRG results (dashed line).

parallel and transverse spin susceptibilities for a magnetic field $h = 0.4T_K$. We see that there is good agreement between the two sets of results. Comparing the differences with those seen in figure 13, where the NRG results are compared with the exact ones, one would conclude that the RPT results are probably the more accurate ones over this range.

The question arises as to whether the RPT results can give similarly good results for higher magnetic field values. As we increase the magnetic field the Kondo effect is suppressed and for extremely large fields the renormalized parameters revert to their bare values as can be seen in the results shown in figure 11. We increase the applied field to test the results over this range of fields. We concentrate on the transverse susceptibility as this can change significantly with magnetic field as we pass from the Kondo regime to the local moment regime, while the parallel susceptibility mainly gets suppressed with increase of field.

In figure 16 we show the imaginary part of the transverse susceptibility for $U/\pi\Delta = 3.0$ for $h = 2T_K$ ($\ln h/T_K = 0.693$). There is quite a dramatic change from the results for $h = 0.4T_K$, shown in figure 15. The spectral weight in the region $\omega < 0$ is almost completely suppressed, and there is a single sharp peak in the spectrum for $\omega > 0$. Again there is remarkable agreement of the RPT results with those obtained from the direct NRG calculations.

For values of the magnetic field such that $\ln(h/T_K) \sim 3.0$, we see from figure 11 that $\tilde{U}(h)$ is enhanced over its bare value U, corresponding to the local moment regime. It is interesting to see whether the Fermi liquid theory can be applied also in this regime. In figure 17 we plot the transverse spin spectral density calculated with the NRG and RPT for $h/T_K = 20$ ($\ln h/T_K = 3.0$). We see that remarkably that there is good agreement in this regime as well: both the peak positions and total spectral weight are in agreement. The peak position corresponds to $0.86 \times 2h$. Though it can be seen from figure 11 that the renormalized field parameter $\tilde{h}(h)$ is enhanced over h, the peak position is not at $2\tilde{h}$, and is somewhat less than the simple Zeeman splitting $2h$. The NRG results are much broader but this is because a discrete spectrum had to be used, and the broadening, which is applied on a logarithmic scale, is much larger at higher values of ω.

Finally, we check the extreme limit, $h/T_K = 10^3$ ($\ln h/T_K = 6.93$, $h = 0.995$), where it can be seen in figure 11 that the renormalized parameters revert to their bare values. Again
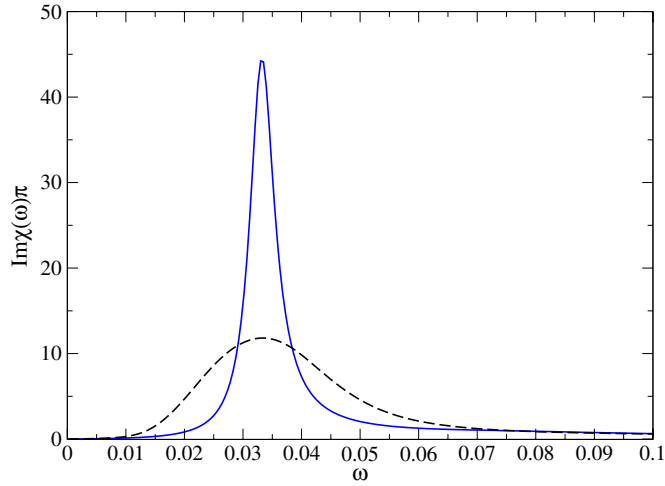
Figure 17. The RPT results for the imaginary parts of $\chi_{s,\perp}(\omega, h)$ (thick full line) for $h = 20T_K$ as a function of ω for $U/\pi\Delta = 3.0$ compared with the NRG results (dashed line).
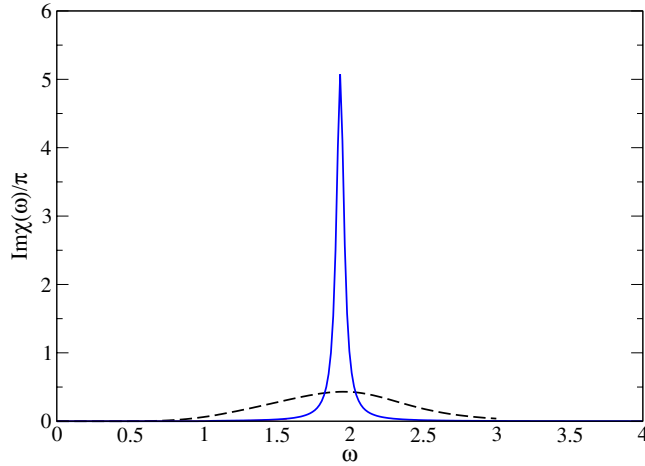

Figure 18. The RPT results for the imaginary parts of $\chi_{s,\perp}(\omega, h)$ (thick full line) for $h = 10^3 T_K$ as a function of ω for $U/\pi\Delta = 3.0$ compared with the NRG results (dashed line).

from the results given in figure 18 it can be seen that the two sets of results correspond. In this regime the peak is at $\omega_p = 2h$, and all many-body effects have disappeared.

The similarity of the parallel susceptibility to the susceptibilities in the absence of a magnetic field suggests that this response function should satisfy the Korringa–Shiba relation. We test this out by plotting the imaginary value of $\chi_\perp(\omega, h)$ divided by $\omega\pi\chi_\perp^2(0, h)$ in figure 19 for $U/\pi\Delta = 3.0$ and $h/T_K = 0.1, 0.4, 1$ (the parallel susceptibility is very much suppressed for larger values of h). We see that the results confirm that there is generalization of the Korringa–Shiba relation for the longitudinal susceptibility in the presence of a magnetic field, and there is a recent paper giving a derivation of this result [20]. In figure 19 it can be seen that increasing the magnetic field broadens the central peak, and this reflects the suppression of
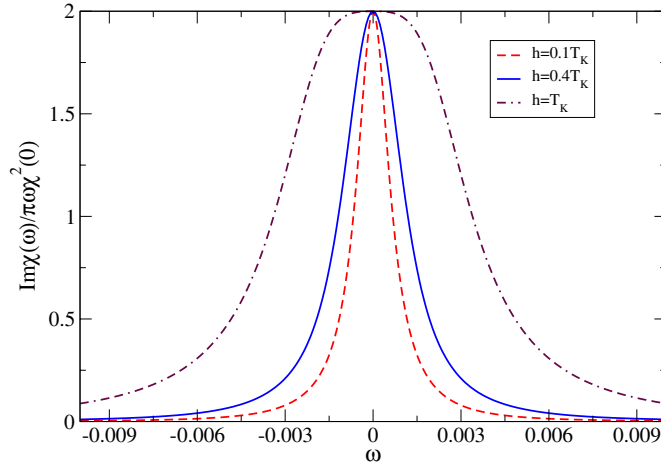
Figure 19. Results for Im $\chi_{s,\parallel}(\omega, h)/\pi \chi_{s,\parallel}^2(0, h)$ calculated using the RPT equations for a range of values of the magnetic field h. The results confirm that there is a generalized Shiba relation [20] for the longitudinal susceptibility in the presence of a magnetic field.

the Kondo resonance. The increase of area under the peak with increasing magnetic field, from equation (18), can be related to the corresponding decrease in the static parallel susceptibility.

4. Conclusions

We have taken into account processes involving repeated quasiparticle scattering to calculate the dynamical charge and spin susceptibilities at zero temperature. As we use the exact irreducible vertices at $\omega = 0$, we know from Fermi liquid theory that the results will be asymptotically exact as $\omega \to 0$, and that the Korringa–Shiba relation will be satisfied. We have also shown that the total spectral weight is given correctly. However, it is not self-evident that taking into account these processes alone in the RPT will constitute a good approximation over all the relevant energy scales. By comparing the results with those obtained by a direct evaluation of the response functions using the NRG we have established that the results of the RPT calculations give a remarkably accurate description of the dynamic spin susceptibilities for the Anderson model with $U > 0$ over all the relevant energy scales and arbitrary values of the external magnetic field. The earlier work of Kuramoto and Miyake [12] came to the same conclusion, though their derivation is restricted to the Kondo limit, and with no magnetic field.

Whereas the spin excitations are enhanced and pushed to lower frequencies for large values of U, the low energy charge excitations are suppressed and pushed to higher energies. The RPT results in this case can only accurately describe the low energy suppression, as the high energy peaks in the charge spectrum are pushed to energies of the order $\omega \sim U/2$, where the low energy renormalized parameters used are not appropriate. It is the spin fluctuations, however, which are the important fluctuations in this regime; they are enhanced and pushed to lower energies. The energy scale of these fluctuations in the large U regime is the Kondo temperature T_K, which is the renormalized energy scale, and over this scale the RPT is an excellent approximation. For the negative U Anderson model the opposite will be the case. For large absolute values of U the spin fluctuations are suppressed and the charge fluctuations enhanced and driven to low energies. In this case it will be the charge fluctuations that are physically the more important ones, and for these the RPT will provide a good description.

In calculating the quasiparticle contribution to the low energy spectral density of the single particle Green's function $G_\sigma(\omega)$, it has to be multiplied by the quasiparticle weight factor z (wavefunction renormalization factor). At first sight it might seem surprising that the quasiparticle contribution to the dynamic susceptibility does not have to be multiplied by a factor z^2. The reason why such a factor is not required is because there is also a renormalization of the vertex $\Lambda(\omega_1:\omega)$ which couples the system to the external magnetic field. It can be shown via a Ward identity that this vertex evaluated at $\omega_1 = \omega = 0$ is equal to $1/z$ [19] and, as a consequence, on differentiating twice with respect to H this brings in a factor $1/z^2$ which cancels factors of z from the product of the full Green's functions. As a result the z does not appear in calculating the dynamical response functions from the RPT.

The fact that the RPT gives good results for over the complete low energy scale ω set by T^* indicates that it should also give a good description of the temperature dependence over the same range, and this is currently being investigated. The approach used here can be generalized to lattice models, such as the Hubbard model and Hubbard–Holstein models, within the dynamical mean field theory, and these calculations are also in progress.

Acknowledgments

Appendix

The free local quasiparticle propagator $\tilde{G}_\sigma(\omega)$ for the symmetric Anderson model, with a magnetic field H acting at the impurity site, is given by

$$\tilde{G}_{d\sigma}(\omega) = \frac{1}{\omega + i\tilde{\Delta}\mathrm{sgn}(\omega) + \sigma\tilde{h}} \tag{29}$$

in the zero temperature perturbation theory formalism. There are two independent quasiparticle pair propagators defined by

$$\tilde{\Pi}_{h\sigma'}^{p\sigma}(\omega, \tilde{h}) = \frac{i}{2\pi} \int_{-\infty}^{\infty} \tilde{G}_\sigma(\omega + \omega', \tilde{h})\tilde{G}_{\sigma'}(\omega', \tilde{h})\, d\omega', \tag{30}$$

and

$$\tilde{\Pi}_{p\sigma'}^{p\sigma}(\omega, \tilde{h}) = \frac{i}{2\pi} \int_{-\infty}^{\infty} \tilde{G}_\sigma(\omega - \omega', \tilde{h})\tilde{G}_{\sigma'}(\omega', \tilde{h})\, d\omega'. \tag{31}$$

These integrals can be evaluated analytically and the results for $\omega > 0$ are

$$\tilde{\Pi}_{h\uparrow}^{p\uparrow}(\omega, \tilde{h}) = \frac{\tilde{\Delta}}{\pi(\tilde{h}^2 + \tilde{\Delta}^2)} \qquad \text{for } \omega = 0,$$
$$= \frac{-\tilde{\Delta}}{\pi\omega(\omega + 2i\tilde{\Delta})} \left\{ \ln\left(\frac{\omega + i\tilde{\Delta} - \tilde{h}}{i\tilde{\Delta} - \tilde{h}}\right) + \ln\left(\frac{\omega + i\tilde{\Delta} + \tilde{h}}{i\tilde{\Delta} + \tilde{h}}\right) \right\}$$
$$\text{for } \omega \neq 0 \tag{32}$$

and

$$\tilde{\Pi}^{p\uparrow}_{h\downarrow}(\omega, \tilde{h}) = \frac{i}{\pi(i\tilde{\Delta} - \tilde{h})} - \frac{1}{2\pi\tilde{\Delta}} \ln\left(\frac{i\tilde{\Delta} - \tilde{h}}{i\tilde{\Delta} + \tilde{h}}\right) \qquad \text{for } \omega = -2\tilde{h},$$

$$= \frac{-i}{\pi}\left\{\frac{1}{\omega + 2\tilde{h} + 2i\tilde{\Delta}} \ln\left(\frac{\omega + i\tilde{\Delta} + \tilde{h}}{i\tilde{\Delta} + \tilde{h}}\right) - \frac{1}{\omega + 2\tilde{h}} \ln\left(\frac{\omega + i\tilde{\Delta} + \tilde{h}}{i\tilde{\Delta} - \tilde{h}}\right)\right\}$$

$$\text{for } \omega \neq -2\tilde{h}. \tag{33}$$

The formulae for $\omega < 0$ are obtained by replacing i with $-i$ in the above. For particle–hole symmetry, we have $\tilde{\Pi}^{p\uparrow}_{p\downarrow}(\omega, \tilde{h}) = -\tilde{\Pi}^{p\downarrow}_{h\downarrow}(\omega, \tilde{h})$, and $\tilde{\Pi}^{p\downarrow}_{h\downarrow}(\omega, \tilde{h}) = \tilde{\Pi}^{p\uparrow}_{h\uparrow}(\omega, \tilde{h}) = \tilde{\Pi}^{p\downarrow}_{h\downarrow}(\omega, -\tilde{h})$.

References

[1] Anderson P W 1961 *Phys. Rev.* **124** 41
[2] Wilson K G 1975 *Rev. Mod. Phys.* **47** 773
[3] Krishnamurthy H R, Wilkins J W and Wilson K G 1980 *Phys. Rev.* B **21** 1003
    Krishnamurthy H R, Wilkins J W and Wilson K G 1980 *Phys. Rev.* B **21** 1044
[4] Hewson A C 1993 *Phys. Rev. Lett.* **70** 4007
[5] Hewson A C 2001 *J. Phys.: Condens. Matter* **13** 10011
[6] Yamada K 1975 *Prog. Theor. Phys.* **53** 970
[7] Hewson A C, Oguri A and Meyer D 2004 *Eur. Phys. J.* B **40** 177
[8] Serene J W and Rainer D 1983 *Phys. Rep.* **101** 222
[9] Kuramoto Y and Kitaoka Y 2000 *Dynamics of Heavy Electrons* (Oxford: Clarendon) chapter 1
[10] Pines D and Noziéres P 1966 *The Theory of Fermi Liquids* vol 1 (New York: Benjamin)
[11] Shiba H 1975 *Prog. Theor. Phys.* **54** 967
[12] Kuramoto Y and Miyake K 1990 *J. Phys. Soc. Japan* **59** 2831
[13] Sakai O, Shimizu Y and Kasuya T 1989 *J. Phys. Soc. Japan* **58** 3666
[14] Costi T A, Hewson A C and Zlatić V 1994 *J. Phys.: Condens. Matter* **6** 2519
[15] Hewson A C 2005 *J. Phys. Soc. Japan* **74** 8
[16] Koller W, Hewson A C and Edwards D M 2006 *Phys. Rev.* B **73** 045117
    (Hewson A C, Bauer J and Koller W 2005 *Preprint* cond-mat/0508465)
[17] Friedel J 1956 *Can. J. Phys.* **54** 1190
    Langer J M and Ambegaokar V 1961 *Phys. Rev.* **164** 498
    Langreth D C 1966 *Phys. Rev.* **150** 516
[18] Hofstetter W 2000 *Phys. Rev. Lett.* **85** 1508
[19] Nozières P 1966 *Theory of Interacting Fermi Systems* (New York: Benjamin)
[20] Garst M, Wölfle P, Borda L, von Delft J and Glazman L 2005 *Phys. Rev.* B **72** 205125